WL-TR-97-1155

DEVELOPMENT OF AN IMPLANT ISOLATION
PROCESS FOR HETEROJUNCTION BIPOLAR
TRANSISTORS

RABI S. BHATTACHARYA

UES, INC.
4401 DAYTON-XENIA ROAD
DAYTON, OH 45432-1894

APRIL 1997

FINAL REPORT FOR 05/03/96-02/02/97

THIS IS A SMALL BUSINESS INNOVATION RESEARCH (SBIR) PHASE I REPORT

APPROVED FOR PUBLIC RELEASE; DISTRIBUTION IS UNLIMITED.

DTIC QUALITY INSPECTED 3

AVIONICS DIRECTORATE
WRIGHT LABORATORY
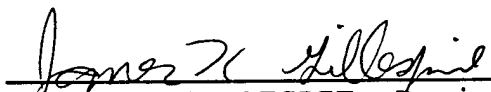AIR FORCE MATERIEL COMMAND
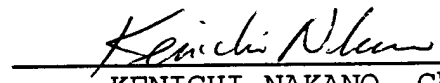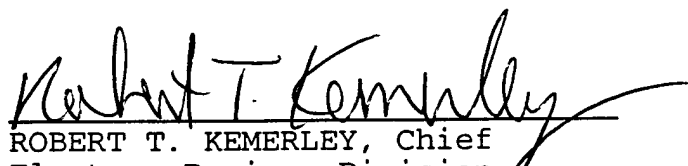WRIGHT PATTERSON AFB OH 45433-7623

19970912 053

NOTICE

USING GOVERNMENT DRAWINGS, SPECIFICATIONS, OR OTHER DATA INCLUDED IN THIS DOCUMENT FOR ANY PURPOSE OTHER THAN GOVERNMENT PROCUREMENT DOES NOT IN ANY WAY OBLIGATE THE US GOVERNMENT. THE FACT THAT THE GOVERNMENT FORMULATED OR SUPPLIED THE DRAWINGS, SPECIFICATIONS, OR OTHER DATA DOES NOT LICENSE THE HOLDER OR ANY OTHER PERSON OR CORPORATION; OR CONVEY ANY RIGHTS OR PERMISSION TO MANUFACTURE, USE, OR SELL ANY PATENTED INVENTION THAT MAY RELATE TO THEM.

THIS REPORT IS RELEASABLE TO THE NATIONAL TECHNICAL INFORMATION SERVICE (NTIS). AT NTIS, IT WILL BE AVAILABLE TO THE GENERAL PUBLIC, INCLUDING FOREIGN NATIONS.

THIS TECHNICAL REPORT HAS BEEN REVIEWED AND IS APPROVED FOR PUBLICATION.

JAMES K. GILLESPIE, Project Eng
Device Technology Branch
Electron Devices Division

KENICHI NAKANO, Chief
Device Technology Branch
Electron Devices Division

ROBERT T. KEMERLEY, Chief
Electron Devices Division
Avionics Directorate

IF YOUR ADDRESS HAS CHANGED, IF YOU WISH TO BE REMOVED FROM OUR MAILING LIST, OR IF THE ADDRESSEE IS NO LONGER EMPLOYED BY YOUR ORGANIZATION PLEASE NOTIFY WL/AADD____WRIGHT-PATTERSON AFB OH 45433-7327 TO HELP MAINTAIN A CURRENT MAILING LIST.

Do not return copies of this report unless contractual obligations or notice on a specific document requires its return.

DTIC QUALITY INSPECTED 3

REPORT DOCUMENTATION PAGE

1. AGENCY USE ONLY (Leave blank)	2. REPORT DATE	3. REPORT TYPE AND DATES COVERED
	APR 1997	FINAL 05/03/96--02/02/97

4. TITLE AND SUBTITLE DEVELOPMENT OF AN IMPLANT ISOLATION PROCESS FOR HETEROJUNCTION BIPOLAR TRANSISTORS

6. AUTHOR(S) RABI S. BHATTACHARYA

5. FUNDING NUMBERS

C F33615-96-C-1876
PE 65502
PR 3005
TA 11
WU EA

7. PERFORMING ORGANIZATION NAME(S) AND ADDRESS(ES)

UES, INC.
4401 DAYTON-XENIA ROAD
DAYTON, OH 45432-1894

8. PERFORMING ORGANIZATION REPORT NUMBER

9. SPONSORING / MONITORING AGENCY NAME(S) AND ADDRESS(ES)

AVIONICS DIRECTORATE
WRIGHT LABORATORY
AIR FORCE MATERIEL COMMAND
WRIGHT PATTERSON AFB OH 45433-7623
POC: JAMES K. GILLESPIE, WL/AADD (937) 255-1874 ext 3459

10. SPONSORING / MONITORING AGENCY REPORT NUMBER

WL-TR-97-1155

11. SUPPLEMENTARY NOTES THIS IS A SMALL BUSINESS INNOVATION RESEARCH (SBIR) PHASE I REPORT.

12a. DISTRIBUTION / AVAILABILITY STATEMENT

APPROVED FOR PUBLIC RELEASE; DISTRIBUTION IS UNLIMITED.

12b. DISTRIBUTION CODE

13. ABSTRACT (Maximum 200 words)

There is great interest in heterojunction bipolar transistors (HBT) for high-speed, high-power electronic devices. The major problem in the fabrication of HBT circuits is the electrical isolation of individual devices in power device design, where it is desirable to have collector and sub-collector layers 1 μm thick or more. The objective of Phase I research was to develop device isolation schedules based on MeV energy O^+ and B^+ implantations. A number of ion implantation schedules based on O^+, $O^+ + Ga^+$, and B^+ implantations have been developed by using computer simulations. These schedules have been tested for the isolation of AlGaAs/GaAs and InGaP/GaAs HBTs. Low leakage currents and high breakdown voltages necessary for the optimum device performance have resulted from selected implantation schedules. Hall measurements were performed after various implantations using single layer n and p-type GaAs of known thickness and carrier concentrations. These data will be useful in optimizing dose levels for the above mentioned ion species for the desired isolation of devices.

14. SUBJECT TERMS

Device Isolation, Ion Implantation, Heterojunction, Bipolar Transistors, High Energy Ions

15. NUMBER OF PAGES

36

16. PRICE CODE

17. SECURITY CLASSIFICATION OF REPORT	18. SECURITY CLASSIFICATION OF THIS PAGE	19. SECURITY CLASSIFICATION OF ABSTRACT	20. LIMITATION OF ABSTRACT
UNCLASSIFIED	UNCLASSIFIED	UNCLASSIFIED	SAR

PREFACE

This technical report has been prepared as part of the requirement of the Phase I SBIR Contract No. F33615-96-C-1876 with the Department of the Air Force, Wright-Patterson Air Force Base, Dayton, OH. The report covers work conducted during the period 3 May 1996 through 2 February 1997 and constitutes the final report under this contract. The Air Force Project Engineer was Mr. James Gillespie (WL/AADD).

ACKNOWLEDGMENT

TABLE OF CONTENTS

LIST OF ILLUSTRATIONS

LIST OF TABLES

1.0 INTRODUCTION

Heterojunction bipolar transistors (HBT) are attracting much interest for high-speed, high-power electronic devices. The major problem in the fabrication of HBT circuits is the electrical isolation of individual devices. An effective isolation would minimize parasitic capacitance and resistance effects between devices and among interconnect metals, transmission lines and passive circuit elements. The particular problem with HBT isolation is the thick epitaxial structures used in power device design, where it is desirable to have collector and sub-collector layers 1 μm thick or more.

Isolation schemes based on mesa etching have several disadvantages. First, the etching and rinsing results in leakage currents across the etched region, and interference is often generated between adjacent devices. Also, interconnect metal step-coverage and lithographic nonuniformities set practical limits on the epitaxial design of power structures. Second, mesa isolation alone does not provide the high inactive area sheet resistance afforded by compensating or lattice damaging implants [1]. Additional ion implant and/or dielectric isolation of interconnect metal from the active mesa sidewalls are required, thus increasing the process complexity. Contact metallizations for the active device often run over the edge of the mesa causing leakage. Thus, this technique becomes more difficult to control as the interdevice dimensions become smaller and smaller. There are also problems of uniformity and undercutting due to non-uniform etch rates.

Isolation schemes based on keV and MeV ion implantation of H^+ and O^+ have been used successfully to isolate HBT structures [2-5]. It is well established that in GaAs-base materials, ion bombardment creates mid gap electron and hole traps which act to compensate both n- and p-type material. In the case of keV O^+ implantation, there are practical limits on the thickness that can be isolated. The thickness of power HBT device structures, ~3 μm, is simply thicker than the range achievable with conventional energy (200 keV) ion implanters. Although H^+ can penetrate thick layers at keV energies, the thermal stability of the isolation produced by H^+

1

implantation is not very good, and the carrier removal efficiency for H^+ is much lower than that of O^+.

A single dose 5 MeV O^+ implant has been shown to isolate thick, ≥ 1.5 μm, HBT structures [4]. However, annealing between 550 and 600°C was required to obtain the desired resistivities. Also, high doses ($\sim 10^{15}$ cm^{-2}) are required to produce an uniform damage profile at a sufficient level over the entire ~ 2 μm to isolate the devices. This increases the cost of processing due to longer implant time.

Some researchers have been using multiple energy and dose MeV O^+ implants for isolation of thick HBT structures [6]. However, the detail parameters of these schemes have not been published.

In order to implement MeV implant-based isolation schemes in the manufacturing of HBTs, it is necessary to develop schemes based on detailed characterizations of devices so that the advantages and limitations of a scheme will be readily available to the manufacturer. UES proposed to develop these schemes based on MeV energy O^+ and B^+ implantation. The use of B^+, if successful, will allow isolation of a thicker layer at a given energy as compared to that of O^+, since B^+ penetrates significantly deeper than the O^+ ions. This can be a major factor in the implementation of this process in the manufacturing of power devices, because lower MeV machines that are more widely available in the industry can be utilized.

2.0   RESEARCH OBJECTIVES

The Phase I technical objectives were to establish GaAs-AlGaAs HBT device isolation schemes based on MeV O^+ and B^+ implantations. Multiple energy and doses were proposed to be used to generate flat damage profiles in GaAs-AlGaAs for thick HBT structures. It was proposed that the isolation schemes will be tested by measuring the leakage current, breakdown voltage and sheet resistance using HBTs fabricated at the Electron Devices Division of the

Avionics Directorate of the Wright Laboratory (WL). The specific objectives in Phase I were as follows:

1. Generate various isolation schemes based on O^+ and B^+ implantations at various energies and doses using computer simulations.

2. Ion implant HBTs fabricated at the WL using the conditions formulated according to computer simulations.

3. Characterize the device isolation by measuring leakage current and breakdown voltage.

4. Evaluate the carrier removal efficiencies of O^+ and B^+ ions by Hall measurements.

3.0   RESEARCH WORK CARRIED OUT

3.1   EXPERIMENTAL DESCRIPTION

3.1.1   Substrate Wafers

We have procured 5 - AlGaAs/GaAs HBT substrate wafers per the following specifications in Table 1.

Also, we have procured 2 single-layer, 1μm thick, (n and p-type) wafers for characterizations of carrier removal efficiency using O^+ and B^+ beams.

Table 1. AlGaAs/GaAs HBT Structure

Layer No.	Description	Composition	Concentration (cm^{-3})	Thickness (Å)
9	n$^+$In$_y$Ga$_{1-y}$As	y=0.50	>1.0E19	300
8	n$^+$In$_y$Ga$_{1-y}$As	y=0 → 0.50	>1.0E19	250
7	n$^+$ GaAs		4.0 - 5.0E18	500
6	n Al$_x$Ga$_{1-x}$As	x=(0.35 → 0)	5.0E17	500
5	n Al$_x$Ga$_{1-x}$As	x=0.35	5.0E17	500
4	pGaAs		4.0E19	700
3	nGaAs		1.0E16	12500
2	n$^+$GaAs		3.0E18	10000
1	Al$_x$Ga$_{1-x}$As	x=0.30	Undoped	3000
Substrate: 3 inch diameter semi-insulating GaAs				

3.1.2 Fabrication of HBTs

HBTs were designed and fabricated at the Electron Devices Division of the Avionics Directorate of the WL in Dayton, OH. Single and multiple emitter finger devices were fabricated with emitter areas ranging from 35 μm^2 to 350 μm^2. The implant mask consists of a 2-3 μm PMGI layer and 2.5 μm evaporated TiAu or plated Au pads. Following implant, the metal is etched away using gold etch and buffered hydrofluoric acid if Ti is used or lifted off using PMGI stripper. The rest of the fabrication process includes base recess etch, base metallization, extrinsic base material trim etch, collector etch and Ohmic deposition, 410°C alloy, pad metallization, planarization and shunt formation.

3.1.3 Ion Implantation

Ion Implantations were carried out at UES by using the Tandetron accelerator. Multiple energy and doses of O$^+$ and B$^+$ were used. A 1D numerical code was used to model the range and straggle of the successive implants. A flat concentration profile based on superposition of Pearson distributions was obtained.

3.2 EVALUATION OF ISOLATION CHARACTERISTICS

Isolation characteristics were studied by measuring sheet resistance, leakage current and breakdown voltage using the device structure described before. Leakage current and breakdown voltage were measured by using 75 µm wide pads separated by 4 µm. At 30 V applied bias, emitter to emitter, base to base and collector to collector leakage currents were measured for various implant schemes.

The carrier concentration and sheet resistance were measured by using Van der Pauw geometry Hall measurements. These measurements were carried out at the facilities of the Avionics Directorate of the WL.

4.0 RESULTS

4.1 DESIGN OF IMPLANTATION SCHEDULES

Implantation schedules for O^+ and B^+ ions were designed on the basis of computer simulations using Profile™ and TRIM™ codes. Profile code provides a quick simulation of range distributions for ions of energy up to 5 MeV and their summation up to 10 implants. TRIM calculations can provide detailed information on range and damage distributions including energy losses, target atom displacements and electronic excitations [7]. Shown below are a few examples of simulations that were run to determine the implantation schedules for isolating HBT devices.

Examples of two different schedules based on O^+ and $O^+ + Ga^+$ implants corresponding to Tables 2 and 3 are shown in Figures 1 and 2, respectively. In the first example, a 4000Å Si_3N_4 mask was used to simulate the conditions used in actual processing of HBTs.

Table 2. Implant Isolation Schedule Based on O^+ Implantation

Species	Energy (MeV)	Dose (cm^{-2})
O^+	0.25	8E11
	0.60	1E12
	1.00	1E12
	1.50	1E12
	2.00	5E11
	2.50	1E12
	3.10	5E11
	3.70	1E12
	4.40	5E11
	5.00	1E12

Table 3. Implant Isolation Schedule Based on $O^+ + Ga^+$ Implantations

Species	Energy(MeV)	Dose(cm^{-2})
O^+	0.25	8E11
	0.50	1E12
	1.00	1E12
	1.50	1E12
	2.50	1E12
	3.70	1E12
	5.00	1E12
Ga^+	0.60	1E12
	1.10	1E12
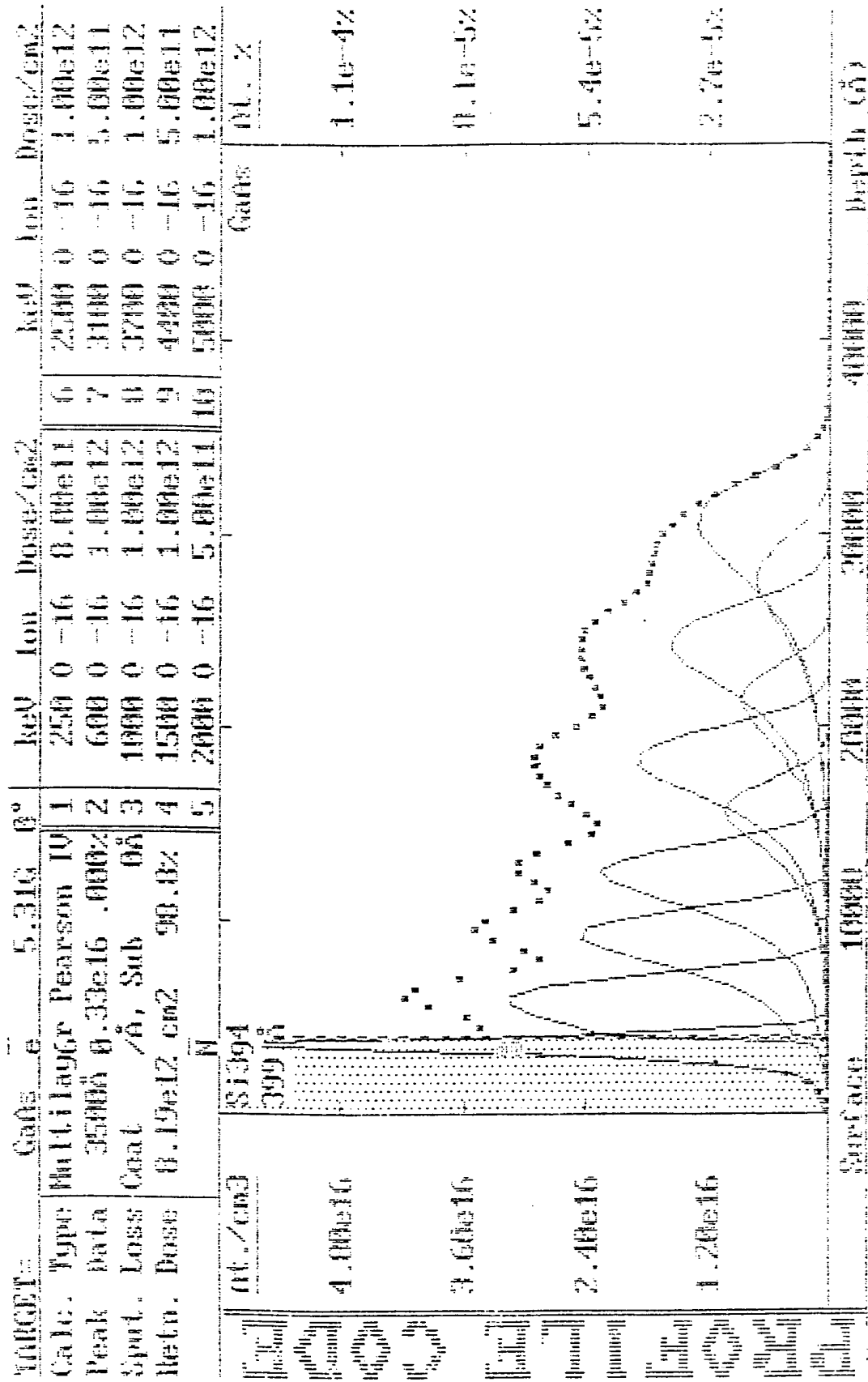
Figure 1. Concentration profiles and their superposition corresponding to Table 2.
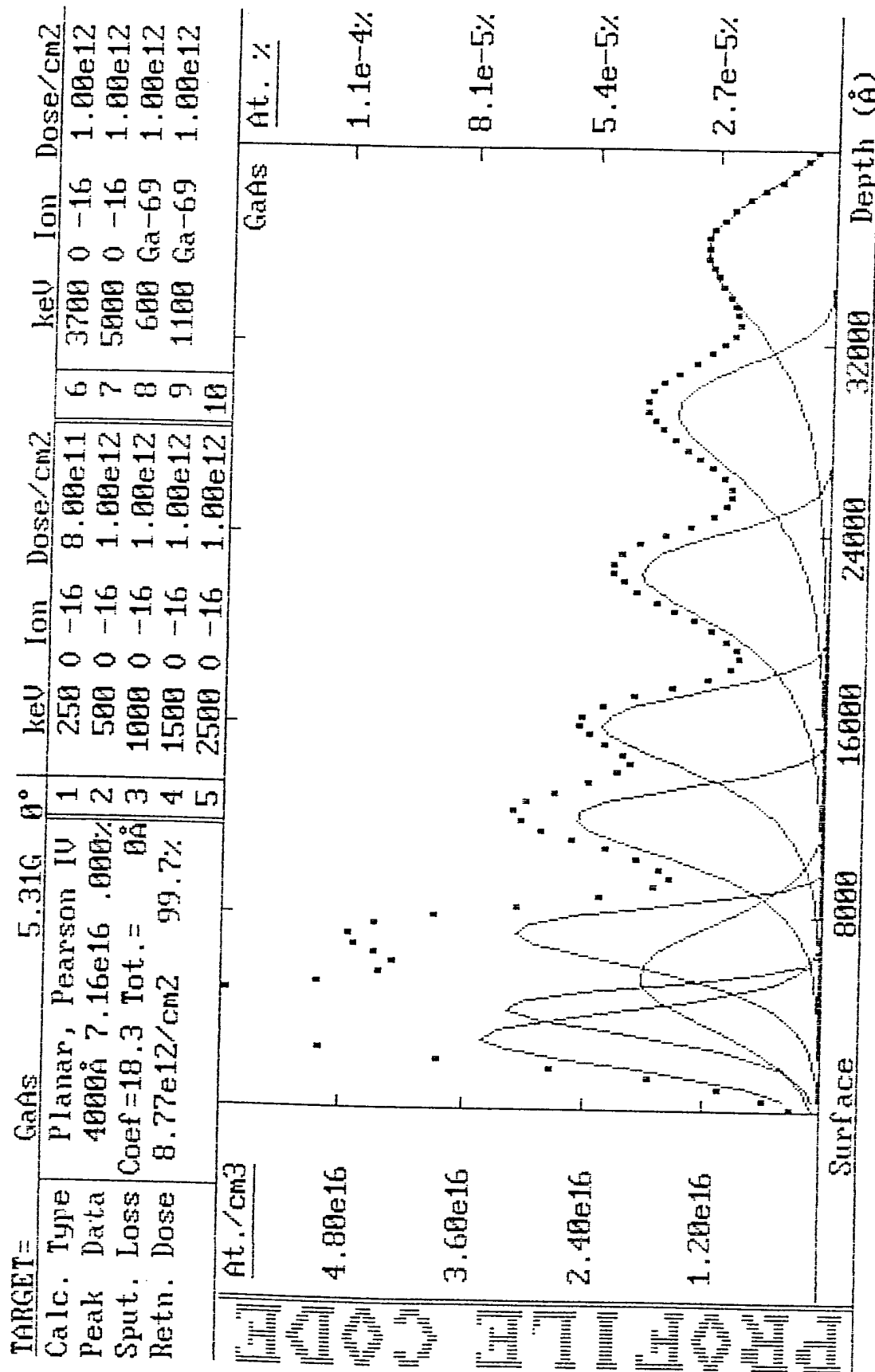
Figure 2. Concentration Profiles and their superposition corresponding to Table 3.

As can be seen from Figures 1 and 2, the sum of these distributions results into a fairly homogeneous distribution of implants. In the first example, the presence of 4000Å Si_3N_4 helped to shift the profiles closer to the GaAs surface. This computer code can simulate only up to 5 MeV. For higher energies up to 6 MeV, as used for oxygen in many cases, TRIM computer code is used to obtain the range and the damage distributions. It was also used to determine the number of displacements per ion as a function of depth using various incoming ions. This information was used to scale the doses necessary to obtain the same level of damage that is responsible for carrier removal.

4.2   ISOLATION OF HBTs USING O^+ AND B^+

HBTs were fabricated at the Avionics Directorate of the WL using the substrate wafers described in Section 3.1.1. In order to compare the quality of device isolation produced by B^+ as opposed to O^+, computer simulations were performed using various energies and doses of B^+ to obtain a similar integrated profile to that of the standard O^+ implantation scheme used for the HBT structure at the Avionics Directorate. In order to determine the B^+ doses necessary to obtain similar carrier removal efficiency as that of O^+, we ran TRIM computer simulations at 1 MeV for both ions in GaAs. The plots of total target displacements as a function of depth obtained from these simulations are shown in Figures 3 and 4. It can be observed that the numbers of displacements/ion/Angstrom at the peak positions of O^+ and B^+ are ~0.3 and ~0.16, respectively. The average vacancy/ion for O^+ and B^+ are 1697 and 1091, respectively. Thus, as a first approximation, we assumed at least a 50% higher dose for B^+ as compared to O^+ for the production of compensating defects. Then, using the Profile™ code, we arrived at the following implantation schedule for B^+ (Table 4) ions that appears to produce a uniform level of damage throughout the layer thickness up to about 4 μm. The profiles of B^+ are shown in Figure 5. The results of characterization of a B^+ implanted wafer are shown in Figure 6.
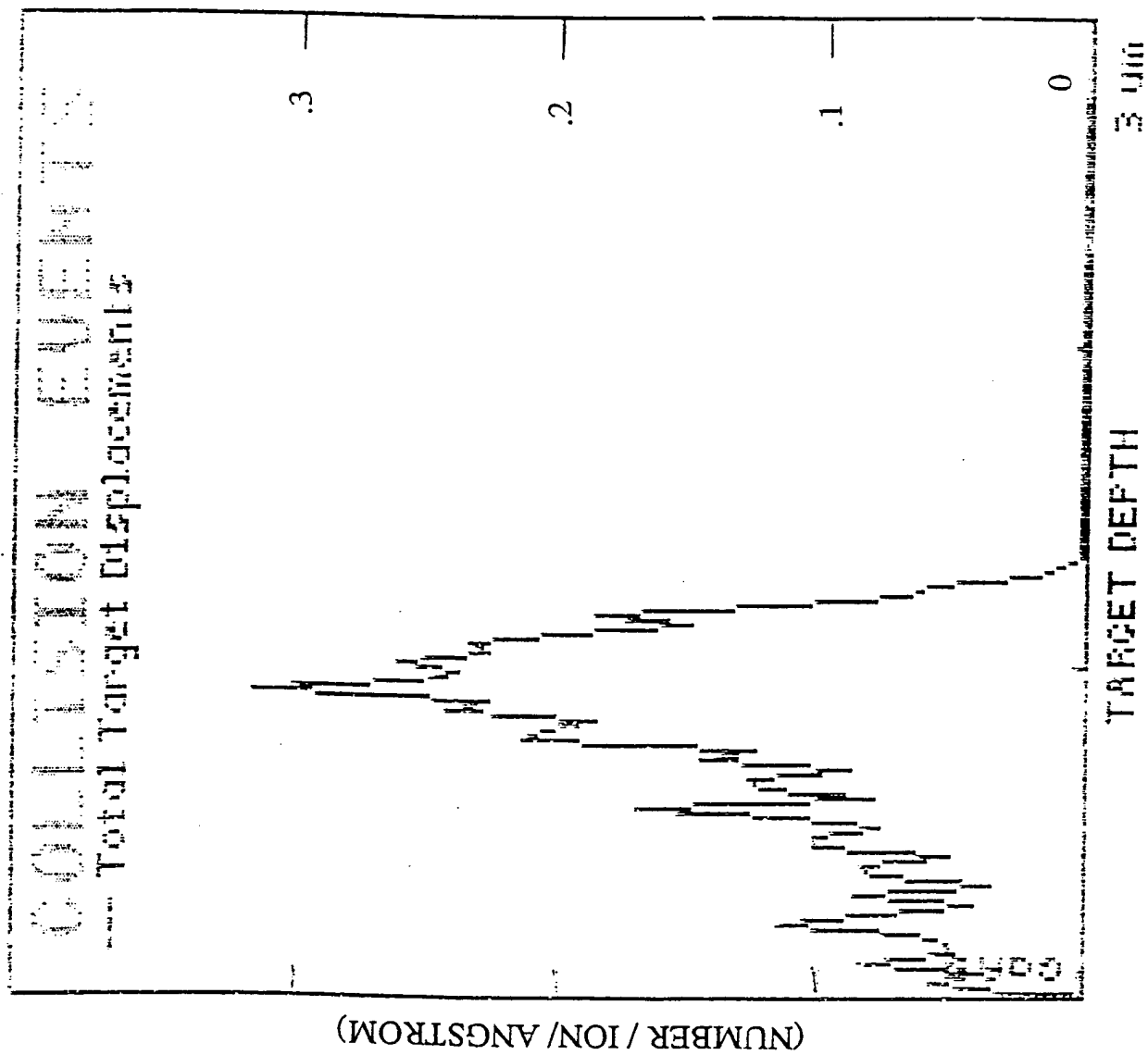
Figure 3. Target displacements as a function of depth for 1 MeV O^+ in GaAs.
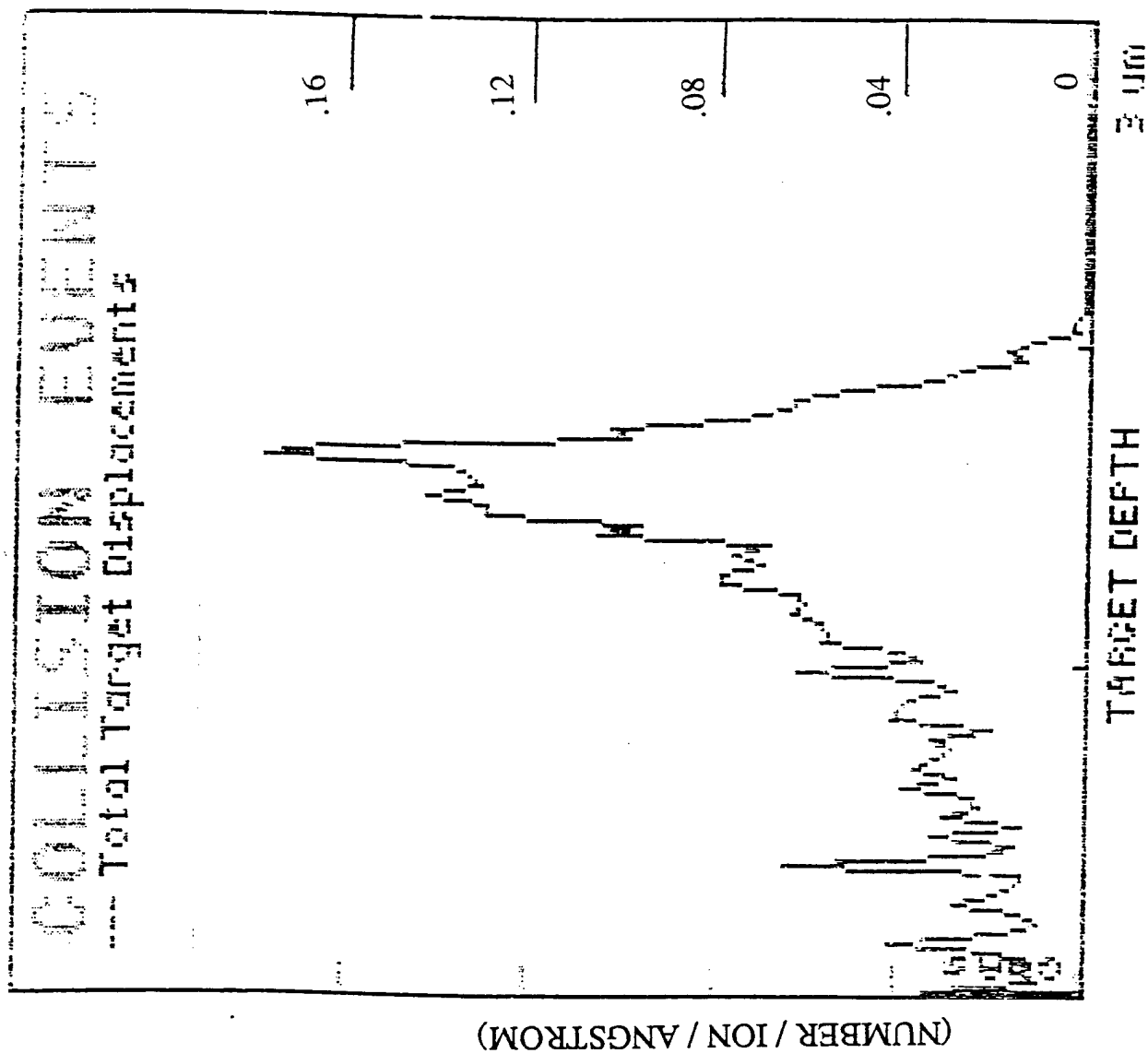
Figure 4. Target displacements as function of depth for 1 MeV B⁺ in GaAs.

11

Table 4. Implantation Schedule for B^+ Ions (UE01)

Energy (MeV)	Dose (cm^{-2})
0.25	1.20E12
0.40	1.50E12
0.70	1.50E12
1.10	1.50E12
1.50	1.50E12
2.00	1.50E12
2.50	1.60E12
3.00	1.70E12
3.50	1.70E12

TARGET= GaAs   5.31G   0"

Calc. Type	Multilayer Pearson IV				keU	Ion	Dose/cm2
Peak Data	4000Å	9.00e16	.000%	6	2000 B	-11	1.30e12
Sputt. Loss Coat	0Å, Sub			7	2500 B	-11	1.60e12
Retn. Dose	1.30e13/cm2	100.0%		8	3000 B	-11	1.70e12
				9	3500 B	-11	1.70e12
				10			

	keU	Ion	Dose/cm2
1	250 B	-11	1.20e12
2	400 B	-11	1.50e12
3	700 B	-11	1.50e12
4	1100 B	-11	1.50e12
5	1500 B	-11	1.50e12

At. %
1.1e-4%
8.1e-5%
5.4e-5%
2.7e-5%

GaAs

Si3N4
3999Å

At./cm3
4.00e16
3.60e16
2.40e16
1.20e16

Surface   10000   20000   30000   40000
Depth (Å)

Figure 5. Concentration profiles of B⁺ in GaAs corresponding to Table 4.

13
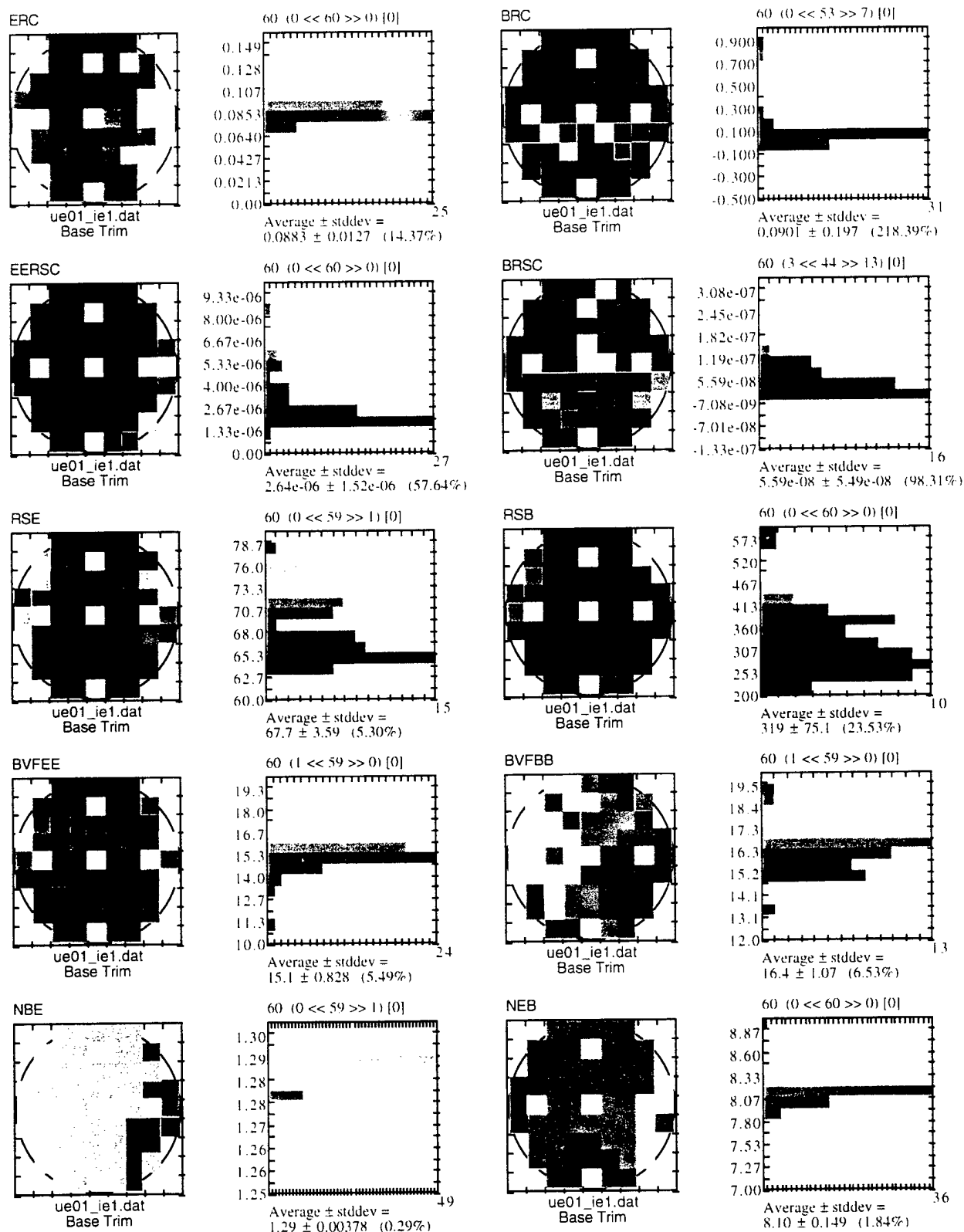
Figure 6a. Results of the characterizations of HBTs isolated by B$^+$ implantations
(a) Before contact alloying.

14
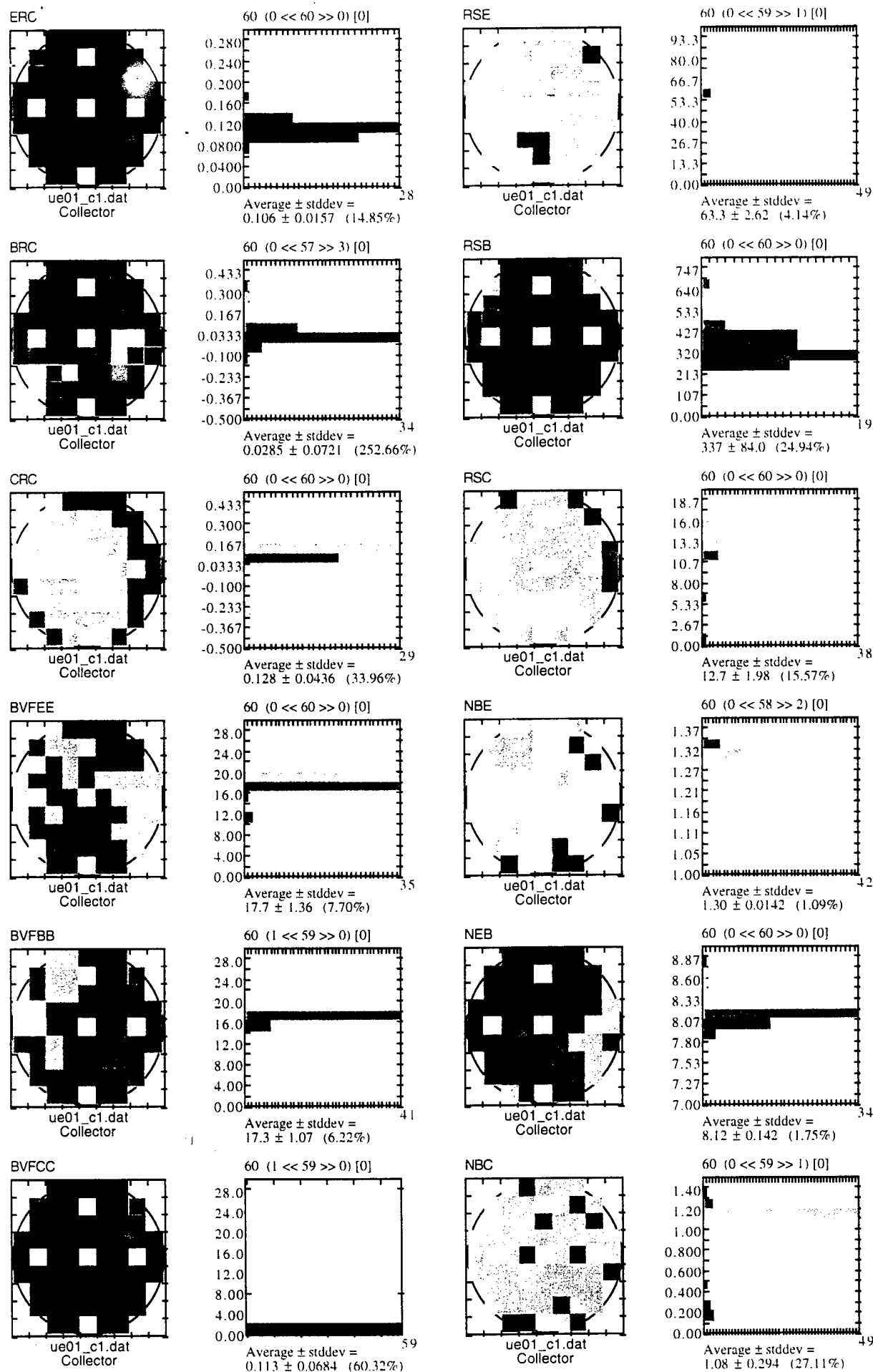
Figure 6b. Results of the characterizations of HBTs isolated by B$^+$ implantations
(b) After contact alloying (400°C).

15

It is clear that, emitter to emitter and base to base breakdown voltages for forcing a 100 μA current is about 17V both before and after the contact annealing (400°C) which is comparable to the results obtained for O^+ implanted wafers. The collector to collector breakdown voltage seems to be lower.

In order to optimize the B^+ implantation schedule, particularly to improve the isolation of collectors, two more implantation schedules including higher energies were designed. These are shown in Table 5 below.

Table 5. Implantation Schedule for B^+ Ions

Energy (MeV)	Dose (cm^{-2}) UE04	Dose (cm^{-2}) UE05
0.25	1.5E12	2.2E12
0.40	1.8E12	2.5E12
0.70	1.8E12	2.5E12
1.10	1.8E12	2.5E12
1.50	1.8E12	2.5E12
2.00	1.8E12	2.5E12
2.50	1.8E12	2.5E12
3.00	1.8E12	2.5E12
3.50	1.8E12	2.5E12
4.00	1.8E12	2.5E12
4.50	1.8E12	2.5E12

HBT wafers UE04 and UE05 were masked to cover half with the boundary perpendicular to the flat and implanted with either O^+ or B^+ schedules. The left half of UE04 and the right half of UE05 were implanted with O^+ according to Table 6. The remaining halves of both wafers were implanted with B^+ schedules according to Table 5.

Table 6. Implantation Schedule for O^+ Ions (UE04 and UE05)

Energy (MeV)	Dose (cm^{-2})
0.25	8E11
0.60	1E12
1.00	1E12
1.50	1E12
2.00	5E11
2.50	1E12
3.10	5E11
3.70	1E12
4.40	5E11
5.10	1E12
5.50	1E12

16

The results of the characterization of UE04 and UE05 are shown in Figure 7. It can be noted that the O^+ implants on UE04 were not effective in isolating the devices. It is not clear whether this is due to the deflection of the beam away from the sample because of malfunction of the deflector power supply or an operator error. However, both B^+ implants, as well as the other O^+ implants, produced comparable results with high breakdown voltages down to collector to collector.

BVFEE

ue04_c1.dat
UE Data 3
DR 250

71 (0 << 71 >> 0) [0]

Average ± stddev =
22.8 ± 14.6 (64.30%)

BVFEE

ue05_c1.dat
UE Data 3
DR 250

71 (0 << 71 >> 0) [0]

Average ± stddev =
37.7 ± 5.86 (15.53%)

BVFBB

ue04_c1.dat
UE Data 3
DR 250

71 (6 << 65 >> 0) [0]

Average ± stddev =
17.8 ± 12.7 (71.60%)

BVFBB

ue05_c1.dat
UE Data 3
DR 250

71 (0 << 71 >> 0) [0]

Average ± stddev =
29.2 ± 2.99 (10.26%)

BVFCC

ue04_c1.dat
UE Data 3
DR 250

71 (9 << 62 >> 0) [0]

Average ± stddev =
18.7 ± 12.8 (68.34%)

BVFCC

ue05_c1.dat
UE Data 3
DR 250

71 (0 << 71 >> 0) [0]

Average ± stddev =
29.4 ± 1.82 (6.18%)

Figure 7. Results of the Characterizations of HBTs Isolated by O^+ and B^+ Implantations.

17

We have also received HBT wafers from Texas Instruments Inc. to develop isolation schemes based on $O^+ + Ga^+$ implantations. The structure of these wafers is shown in Figure 8.

1000Å Si_3N_4
1000Å GaInAs
1500Å GaAs
1000Å InGaP
800Å GaAs
1.1 µm collector
1 µm sub-collector
GaAs

Figure 8. Structure of InGaP/GaAs HBT.

An implantation schedule (Table 7) was developed based on computer simulation:

Table 7. Implantation Schedule Using $O^+ + Ga^+$ for TI Sample

Wafers	Species	Energy (MeV)	Dose (cm^{-2})
All	Oxygen	0.25	8E11
		0.50	1E12
		0.75	5E11
		1.00	1E12
		1.50	1E12
		2.00	5E11
		2.50	1E12
		3.10	5E11
		3.70	1E12
		4.40	5E11
		5.10	1E12
		5.50	1E12
	Gallium	0.60	1E12
		1.10	1E12

Using single finger devices, collector to collector leakage current was measured at 20V applied bias. Leakage currents averaging less than 3 μA was measured using this scheme. The previous schedule that they were using did not include the underlined energies and doses. The previous schedule resulted in leakage currents higher than 300 μA.

4.3   HALL MEASUREMENTS

Hall measurements were performed to determine the carrier removal efficiencies for both $O^+ + Ga^+$ and B^+ implantations. Layers (1 μm thick) of N and P-type with carrier concentrations of 1×10^{19} and 5×10^{19}, respectively, were grown on SI GaAs, and used as the starting materials. Samples of sizes 0.5 cm × 0.5 cm were prepared and were implanted using three different schedules as shown below:

Schedule 1

Species	Energy (MeV)	Dose (cm^{-2})
O^+	0.25	8E11
	0.50	1E12
	1.00	1E12
	1.50	1E12
	2.50	1E12
	3.70	1E12
Ga^+	0.60	1E12
	1.10	1E12

Schedule 2

Species	Energy (MeV)	Dose (cm^{-2})
O^+	0.25	8E11
	0.50	1E12
	1.00	1E12
	1.50	1E12
	2.00	5E11
	2.50	1E12
	3.10	5E11
	3.70	1E12
Ga^+	0.60	1E12
	1.10	1E12

19

Species	Energy (MeV)	Dose 1 cm^{-2}	Dose 2 cm^{-2}	Dose 3 cm^{-2}
B$^+$	0.25	8E11	1.2E12	1.5E12
	0.40	1E12	1.5E12	2.0E12
	0.70	1E12	1.5E12	2.0E12
	1.10	1E12	1.5E12	2.0E12
	1.50	1E12	1.5E12	2.0E12

The results of Hall measurements are summarized below for both N and P-type samples (Table 8 and 9):

Table 8. Results of Hall Measurements of N-type Samples

	As Received	Schedule 1	Schedule 2	Schedule 3		
				Dose 1	Dose 2	Dose 3
Concentration (cm^{-3})	7.09×10^{18}	2.4×10^{15}	1.1×10^{16}	1.74×10^{17}	3.23×10^{16}	8.2×10^{16}
ρ (Ohm-cm)	4.55×10^{-4}	1.9×10^2	9.34×10^1	2.3×10^{-1}	3.4	6×10^{-1}
μ (cm^2/V-sec)	1.94×10^3	1.34×10^1	6.0	1.56×10^2	5.68×10^1	1.27×10^2
I (Amp)	1.8×10^{-2}	3×10^{-7}	2×10^{-6}	3×10^{-4}	2×10^{-5}	10^{-4}

Table 9. Results of Hall Measurements of P-type Samples

	As Received	Schedule 1	Schedule 2	Schedule 3		
				Dose 1	Dose 2	Dose 3
Concentration (cm^{-3})	3.69×10^{19}	1.47×10^{18}	1.25×10^{18}	3.28×10^{19}	9.33×10^{18}	4.7×10^{18}
ρ (Ohm-cm)	1.88×10^{-3}	5.4×10^{-1}	1.5	1.33×10^{-2}	2.4×10^{-2}	5.48×10^{-2}
μ (cm^2/V-sec)	9.01×10^1	7.8	3.33	1.43×10^1	2.78×10^1	2.4×10^1
I (Amp)	1.8×10^{-2}	1×10^{-4}	5×10^{-5}	1.8×10^{-2}	4×10^{-3}	1×10^{-3}

The schedules for O$^+$ + Ga$^+$ used in this investigation were the same as the one that was successfully used for HBT device isolations. The schedule for B$^+$, Dose 2, was also the same as that used for the isolation of HBT wafer UE01. Clearly the carrier concentrations after

implantations using various schedules are about 2-3 orders of magnitude lower for N-type and about one order of magnitude lower for P-type than the as received samples. One would expect a much lower carrier concentrations after implantations based on the results of leakage currents and breakdown voltage of HBT devices. This can be explained from the fact that no masks were used in these samples that resulted in a relatively undamaged layer of about 2000Å near the surface. A cap layer of Si_3N_4 of appropriate thickness, as used in HBT processing, will bring the damage distribution closer to the surface.

In continuation of that work, we have performed Hall measurements on samples implanted through a Si_3N_4 layer. Same N- (1×10^{19} cm^{-3}) and P-type (5×10^{19} cm^{-3}) layers, 1 µm thick, on SI GaAs were used for these implantations. A 4300Å thick Si_3N_4 layer was deposited on these samples using the facilities of Avionics Directorate (J. Sewel). Following implantation schedules based on O^+ and B^+ were used for the carrier removal studies.

Schedule 1

Species	Energy (MeV)	Dose (cm^{-2})
O^+	0.25	8E11
	0.50	1E12
	1.00	1E12
	1.50	1E12
	2.50	5E11

Schedule 2

Species	Energy (MeV)	Dose (cm^{-2})
B^+	0.25	1.2E12
	0.40	1.5E12
	0.70	1.5E12
	1.10	1.5E12

Computer simulations of these implant schedules in 4300Å Si_3N_4 coated GaAs are shown in Figures 9 and 10. As can be seen from these figures, the Si_3N_4 layer has helped in bringing the profile closer to the GaAs surface for both O^+ and B^+. The energies and doses in the schedule 1 are the same as that used in HBT isolations at the Avionics Directorate, except that higher energies and doses were not used since the layer is only 1 µm thick. The B^+ implant schedule is also the same as the part of the schedule used for isolating HBT wafer UE01 that exhibited high emitter to emitter and base to base breakdown voltages.

The results of Hall measurements after stripping the Si_3N_4 layer are summarized below for both N- and P-type samples (Tables 10 and 11).

Table 10. Results of Hall Measurements of N-type Samples Implanted Through Si_3N_4

	As Received	O^+ Implanted Schedule 1	B^+ Implanted Schedule 2
Concentration (cm^{-3})	7.09×10^{18}	7.7×10^{12}	2.62×10^{14}
ρ (Ohm-cm)	4.55×10^{-4}	7.64×10^{2}	6.78×10^{1}
R_s (Ω/□)	4.55	7.64×10^{6}	6.75×10^{5}
µ (cm^2/V-sec)	1.94×10^{3}	1.06×10^{3}	3.52×10^{2}

Table 11. Results of Hall Measurements of P-type Samples Implanted Through Si_3N_4

	As Received	O^+ Implanted Schedule 1	B^+ Implanted Schedule 2
Concentration (cm^{-3})	3.69×10^{19}	1.06×10^{19}	1.02×10^{19}
ρ (Ohm-cm)	1.88×10^{-3}	4.30×10^{-2}	2.17×10^{-2}
R_s (Ω/□)	1.88×10^{1}	4.3×10^{2}	2.17×10^{2}
µ (cm^2/V-sec)	9.01×10^{1}	1.37×10^{1}	2.82×10^{1}

TARGET= GaAs   5.31G   0°

Calc. Type	Multilayer Pearson IV		keV	Ion	Dose/cm2		keV	Ion	Dose/cm2
Peak Data	3750Å 7.37e16 .000%	1	250	0 -16	8.00e11	6			
Sput. Loss	Coat 0Å, Sub 0Å	2	500	0 -16	1.00e12	7			
Retn. Dose	4.26e12/cm2 99.1%	3	1000	0 -16	1.00e12	8			
		4	1500	0 -16	1.00e12	9			
		5	2000	0 -16	5.00e11	10			

At./cm3 | At. %
1.04e17 | 2.4e-4%
7.80e16 | 1.8e-4%
5.20e16 | 1.2e-4%
2.60e16 | 5.9e-5%

Si3N4 4299Å

Surface — GaAs — Depth (Å)

5000   10000   15000   20000
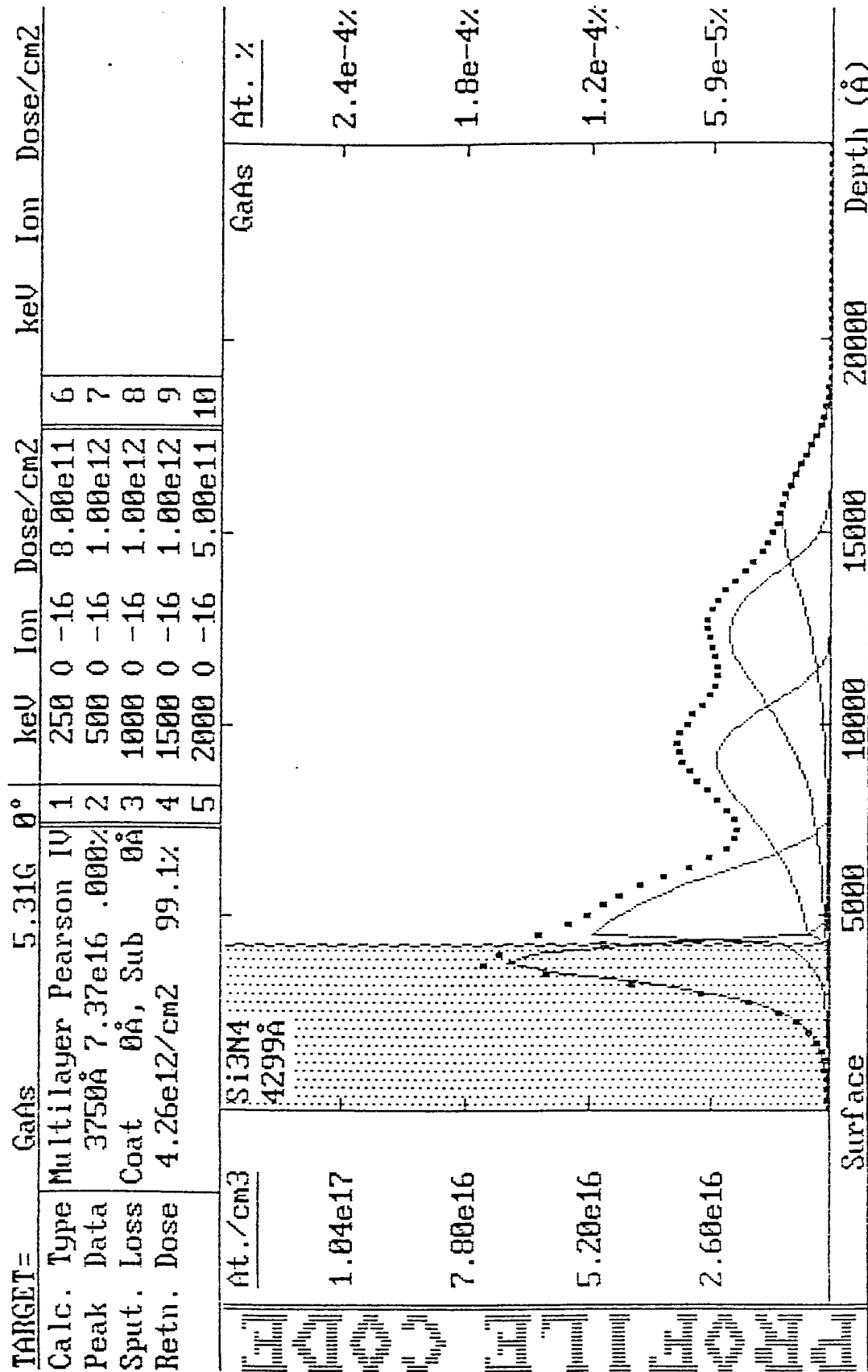
Figure 9.   Concentration Profiles of O$^+$ Ions in 4300Å Si$_3$N$_4$ Capped GaAs According to Schedule 1.

23

TARGET= GaAs 5.31G θ°

			keV	Ion	Dose/cm2		keV	Ion	Dose/cm2
Calc.	Type	Multilayer Pearson IV	1				250	B -11	1.20e12	6
Peak	Data	4500Å 1.17e17 .000%	2				400	B -11	1.50e12	7
Sput.	Loss	Coat 0Å, Sub 0Å	3				700	B -11	1.50e12	8
Retn.	Dose	5.62e12/cm2 98.6%	4				1100	B -11	1.50e12	9
			5							10

At./cm3	At. %
1.36e17	3.1e-4%
1.02e17	2.3e-4%
6.80e16	1.5e-4%
3.40e16	7.7e-5%

Si3N4 4299Å   GaAs

Surface   5000   10000   15000   20000   Depth (Å)
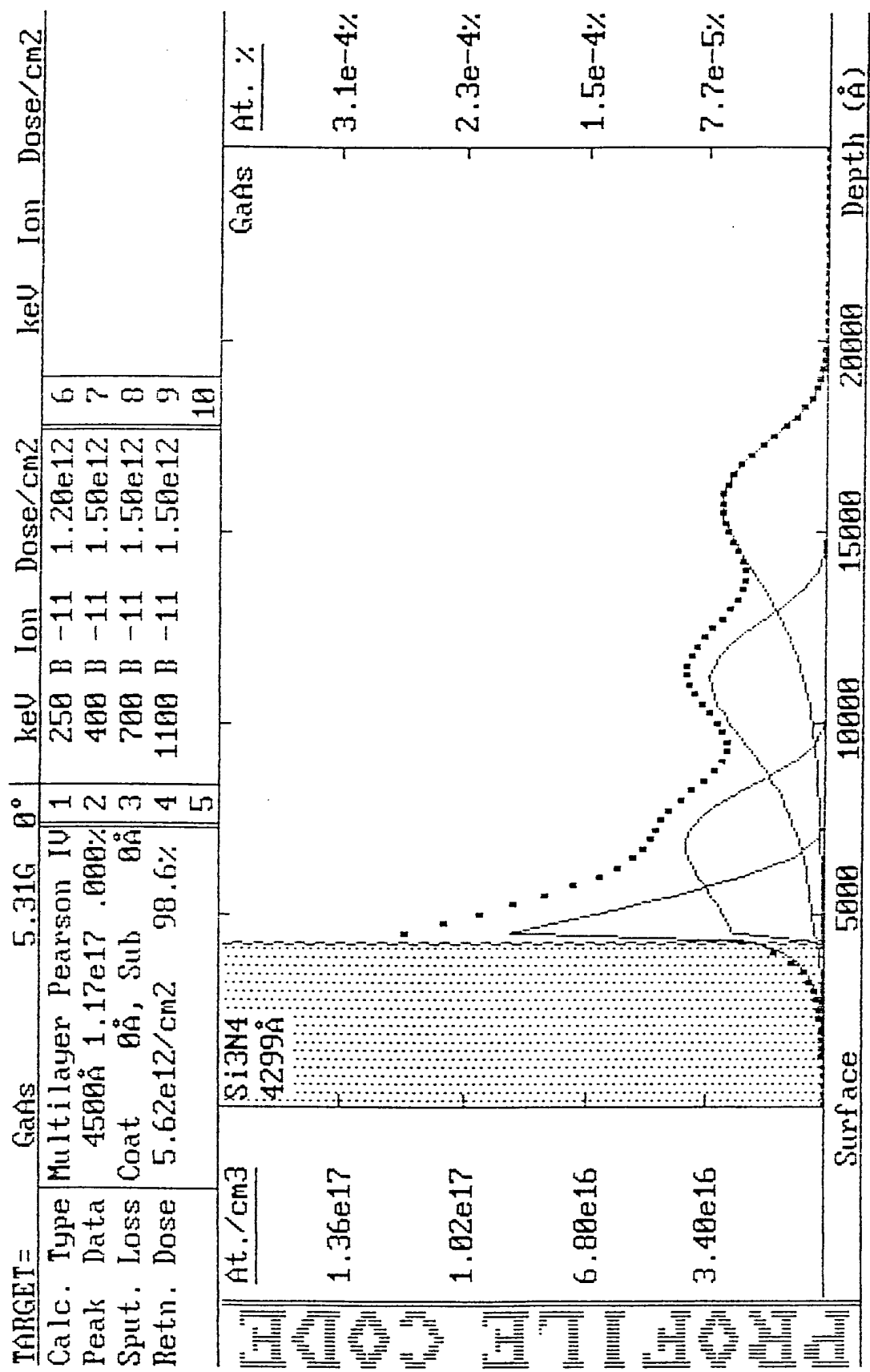
Figure 10. Concentration Profiles of B^+ Ions in 4300Å Capped GaAs According to Schedule 2.

The results in Tables 10 and 11 clearly reveal the importance of placing the damage profile in appropriate depth of the doped layer for efficient removal of carriers.

It should be noted that the carrier concentration for n-type material was reduced by about 6 orders of magnitude by O^+ implantation and 4 orders of magnitude for B^+ implantation. The optimization of implantation parameters for B^+ may result in further reduction of carrier concentration. For p-type material, however, the reduction in carrier concentration for both O^+ and B^+ is about the same, a factor of 3, which is much lower than that of n-type material.

In order to reproduce the results and further optimize the dose schedule required for efficient device isolation, we have evaluated the following implantation schedules.

Schedule 1

Species	Energy (MeV)	Dose (cm^{-2})
O^+	0.25	8E11
	0.50	1E12
	1.00	1E12
	1.50	1E12
	2.50	5E11

Schedule 2

Species	Energy (MeV)	Dose (cm^{-2})
O^+	0.25	8E12
	0.50	1E13
	1.00	1E13
	1.50	1E13
	2.00	5E12

Schedule 3

Species	Energy (MeV)	Dose (cm^{-2})
B$^+$	0.25	2E12
	0.40	2E12
	0.70	2E12
	1.10	2E12
	2.50	5E11

Schedule 4

Species	Energy (MeV)	Dose (cm^{-2})
B$^+$	0.25	3E12
	0.40	3E12
	0.70	3E12
	1.10	3E12

Schedule 5

Species	Energy (MeV)	Dose (cm^{-2})
B$^+$	0.25	8E12
	0.40	1E13
	0.70	1E13
	1.10	1E13

The 1 μm thick n and p-type GaAs samples were coated with 4000 Å Si_3N_4 film prior to the above implantations.

The results of Hall measurements are listed in Tables 12 and 13 for n and p-type samples, respectively.

26

Table 12. Results of Hall Measurement of N-Type Samples Implanted with O^+ and B^+

	O^+ Sch 1	O^+ Sch 2	B^+ Sch 3	B^+ Sch 4	B^+ Sch 5
Concentration (cm^{-3})	1.2×10^{13}	2.2×10^{15}	6.7×10^{12}	1.2×10^{12}	6.7×10^{14}
ρ (Ohm-cm)	8.4×10^{2}	4.7×10^{1}	2×10^{2}	1×10^{3}	3.5×10^{2}
R_s ($\Omega/\square$)	8.46×10^{6}	4.7×10^{5}	2×10^{6}	1×10^{7}	3.5×10^{6}
μ (cm^2/V-sec)	6.1×10^{3}	6×10^{1}	4.6×10^{3}	5.2×10^{3}	2.7×10^{1}

Table 13. Results of Hall Measurement of P-Type Samples Implanted with O^+ and B^+

	O^+ Sch 1	B^+ Sch 3	B^+ Sch 4
Concentration (cm^{-3})	1×10^{19}	6.7×10^{18}	2.6×10^{18}
ρ (Ohm-cm)	4.8×10^{-2}	4.3×10^{-2}	2.4×10^{-1}
R_s ($\Omega/\square$)	4.8×10^{2}	4.3×10^{2}	2.4×10^{3}
μ (cm^2/V-sec)	1.3×10^{1}	2.2×10^{1}	9.97

It should be noted that the O^+ schedule 1 is the part of the same schedule that is being used successfully at the Avionics Directorate to isolate the HBT devices. A factor of 10^6 reduction in carrier concentration in n-type GaAs was obtained by using this implantation schedule. However, for p-type, only a factor of 4 reduction in carrier concentration was obtained. Similar results were found earlier using different samples. Thus, the results are reproducible.

It is clear from Table 12 that B^+ schedules 2 and 3 produced slightly higher reduction in the carrier concentration for both n and p-type samples as compared to that of O^+ schedule 1. The B^+ schedules 3 and 4 consist of a factor of 2 and 3 higher doses at various energies than the

lower reduction in carrier concentration. Thus, the optimum doses for O^+ and B^+ for device isolation should lie close to that in schedules 1 and 3, respectively.

5.0 ESTIMATE OF TECHNICAL FEASIBILITY OF POTENTIAL APPLICATIONS

In Phase I, the feasibility of using high energy O^+ and B^+ ions for the isolation of HBT devices has been demonstrated. After successful completion of Phase II, UES will patent the isolation schemes. These schemes will then be made available to HBT manufacturers or other independent implant houses under licensing agreements for implementation.

Also, UES will upgrade its current MeV implanter beam line and target chamber to accommodate 4" wafers for implantation at high energies. We will be able to process over 50 wafers in an 8-hour shift. By running two or three shifts, we can increase the thruput to 100 or 150 wafers a day. This will allow UES to enter into the implant isolation service business for HBT manufacturing. UES already has contacts with major players among the power HBT manufacturers such as Texas Instruments and Northrop-Grumman.

The expansion of UES capability and availability of a reliable source for implantation will provide support to the ongoing effort of commercialization of power HBTs by various manufacturers in the industry.

HBTs can be used for ultrahigh speed digital circuits, microwave mixers and oscillators, high efficiency microwave power amplifiers, broad band analog circuits such as feedback amplifiers and analog to digital converters.

6.0 SUMMARY

There is great interest in heterojunction bipolar transistors (HBT) for high-speed, high-power electronic devices. The major problem in the fabrication of HBT circuits is the electrical isolation of individual devices in power device design, where it is desirable to have collector and

isolation of individual devices in power device design, where it is desirable to have collector and sub-collector layers 1 μm thick or more. Ion implntation can be used to produce mid-gap electron and hole traps which act to compensate for both n and p-type materials. The objective of Phase I research was to develop device isolation schedules based on MeV energy O^+ and B^+ implantations. A number of ion implantation schedules based on O^+, $O^+ + Ga^+$, and B^+ implantations have been developed by using computer simulations. These schedules have been applied in the isolation of AlGaAs/GaAs and InGaP/GaAs HBTs. O^+ and $O^+ + Ga^+$ implantations resulted in low leakage currents and high breakdown voltages necessary for the optimum device performance. Implantation schedule based on B^+, developed for the first time in this Phase I program, showed comparable low leakage currents and high breakdown voltages before and after the contact annealing. The benefit of using B^+ over O^+ is the 30% higher penetration depth for the same energy that will allow the isolation of thicker HBT structure if desired. Hall measurements have been performed by using some of the computer generated O^+, $O^+ + Ga^+$ and B^+ implanted schedules on single layer n and p-type GaAs layers of known thickness and carrier concentrations. These data will be useful in defining dose levels for the above mentioned ion species for the desired isolation of devices.

HBTs fabricated using the technology developed in Phase I and II can be used for ultrahigh speed digital circuits, microwave mixers and oscillators, high efficiency microwave power amplifiers, broad band analog circuits such as feedback amplifiers and analog to digital converters.

REFERENCES

1. R Williams, Modern GaAs Processing Methods, (Artech House, Boston, 1990), chap.10.
2. F. Ren, S.J. Pearton, W.S. Hobson, T.R. Fullowan, J. Lothian, and A.W. Yanof, Appl. Phys. Lett. 56, 860 (1990).
3. S.J. Pearton, F. Ren, P.W. Wisk, T.R. Fullowan, R.F. Kofp, J.M. Kuo, W.S. Hobson and C.R. Abernathy, J. Appl. Phys. 69, 698 (1991).

5. S.J. Pearton, F. Ren, J.R. Lothian, T.R. Fullowan, A. Katz, P.W. Wisk, C.R. Abernathy, R.F. Kopf, R.G. Elliman, M.C. Ridgway, C. Jagdish, and J.S. Williams, J. Appl. Phys. 71, 4949 (1992).

6. J. Barrette, M. Mack, C. Bozada, R. Dettmer, R. Fitch, J. Sewell, T. Jenkins, and A. W. McCormick, "Improved Oxygen Implant Isolation Process for HBTs" Presented at the GaAs Mantech Conference, 1995.

7. J.P. Biersack and L.G. Haggmark, Nucl. Instrum. Methods 174, 257 (1980).